Journal of Materials Chemistry A

Accepted Manuscript

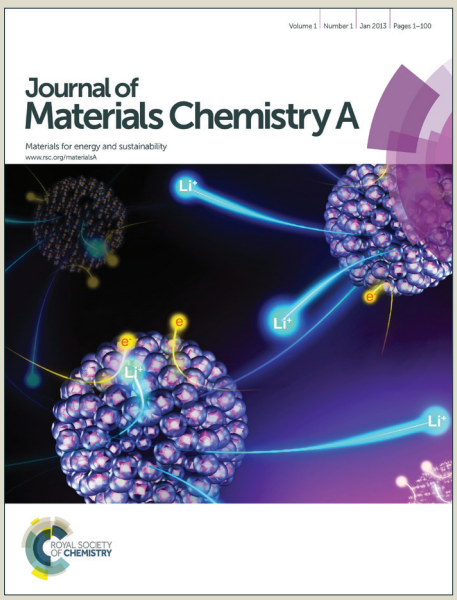

ROYAL SOCIETY OF CHEMISTRY

www.rsc.org/materialsA

Cite this: DOI: 10.1039/c0xx00000x

www.rsc.org/xxxxxx

ARTICLE TYPE

Inkjet Printing $CH_3NH_3PbI_3$ on Mesoscopic TiO_2 Film for Highly Efficient Perovskite Solar Cells

Shao-Gang Li,[a] Ke-Jian Jiang,[a] * Mei-Ju Su,[a,b] Xue-Ping Cui,[a,b] Jin-Hua Huang,[a] Qian-Qian Zhang,[a,b] Xue-Qin Zhou,[b] * Lian-Min Yang,[a] Yan-Lin Song [a] *

Received (in XXX, XXX) Xth XXXXXXXXX 20XX, Accepted Xth XXXXXXXXX 20XX
DOI: 10.1039/b000000x

Inkjet printing technique is successfully used to deposit perovskite $CH_3NH_3PbI_3$ layer on a mesoscopic TiO_2 film. With the combined optimization of the table temperature and the ink composition, a flat and uniform perovskite layer is realized on the TiO_2 film, and the corresponding photovoltaic device exhibits a high efficiency of 12.3% with an average value of 11.2% under AM 1.5G conditions. The current work demonstrates that the inkjet printing method is environmentally benign and cost-effective with reduced waste of the toxic Pb-containing materials encountered inevitably in the existing techniques during the device preparation.

Introduction

During the past two decades, there have been extensive investigations for cost-effective thin film solar cells as alternative technologies to conventional inorganic counterparts. Among the innovative technologies, the perovskite solar cell based on hybrid organometal trihalide perovskites, in the form of (MA)[PbX_3] (MA = $CH_3NH_3^+$; X = Cl, Br, or I), is emerging as a strong competitor, and the power conversion efficiency (*PCE*) rapidly rosed from 3.8% to more than 16% in the last five years.[1-13] Recently, Recently, a certified PCE of 17.9% was reported by the national renewable energy laboratory (NREL).[14] In addition, higher efficiency of 19.3 % was also reported by Yang′s group.[15] In this solar cell, high crystallinity perovskite layers can be formed by simple spin coating method, functioning as desirable light absorbers with a direct and tunable band-gap. As ideal photovoltaic materials, they possess both high hole and electron transport ability, small exciton binding energy (~20 meV), and long carrier diffusion lengths (100–1000 nm).[16,17] At present, most of the perovskite layers were deposited on planar or mesoscopic metal oxide substrates by spin coating technique with one-step or two-step approach.[1-7,9-13] Alternatively, vacuum deposition technique was also employed to generate high flat and uniform perovskite film, exhibiting a *PCE* up to 15.4%.[8,18] In the perovskite solar cells, photovoltaic performance is greatly dependent on the perovskite film morphology, which is relied on deposition method, annealing process and additives employed.[19-28] Despite enormous progress made in the device design and performance, exploring suitable printing technique for the controlable and scalable production of the perovskite layers is highly expected when considering their practical applications. To this end, an ultra-sonic spray-coating technique was employed for the fabrication of planar heterojunction perovskite solar cells, exhibiting a high power conversion efficiency *PCE* of 11% with an average *PCE* of 7.3%.[29] Recently, two-step method including spin-coating and inkjet printing processes were used for fabricating the perovskite film, delivering an efficiency of 11.60%.[30]

Inkjet printing is a material-conserving deposition technique used for control deposition of different materials dispersed or dissolved in solution, enabling easy and fast deposition of functional materials on various substrates with large-area.[31] Inkjet printing has been a popular choice in the fabrication of various optoelectonic devices including light-emitting devices, solar cells and field-effect transistor.[32-34] In the previous report, polymer:fluorine bulk heterojunction organic photovoltaics were fabricated by the technique, and some critical parameters, including solvent formulation and inkjet table temperatures, were studied to achieve high-quality inject printed photoactive layers.[33]

In this work, the perovskite $CH_3NH_3PbI_3$ film was deposited as a light absorber on mesoscopic TiO_2 film for the perovskite solar cells by means of inkjet printing technique. The printing ink contains the perovskite precursor methylammonium iodide (MAI) and lead iodide (PbI_2) dissolved in γ-butyrolactone. We investigated the effect of the printing table temperature on the morphology and structure of the perovskite film and the device performance. We further investigated the role of the methylammonium chloride (MACl) as an additive used in the ink on the film morphology and the device performance. Combined optimization of both the parameters, a flat and uniform perovskite layer on the mesoscopic TiO_2 film was realized. The film has strong light harvesting capacity, and the corresponding device exhibited a high power conversion efficiency of 12.3% with an average value of 11.2% under AM 1.5 illumination. Our results demonstrate that inkjet printing technique is an effective fabrication tool for highly efficient perovskite solar cells. More importantly, the drop-on-demand inkjet technique is environmentally friendly for the deposition of the perovskite film. In contrast, a considerable amount of toxic Pb-containing materials is discarded in the fabrication processes of the existing spin coating, spray coating, and vacuum deposition.

Results and discussion

In our experiments, all the samples were built on transparent

fluorine-doped tin-oxide (FTO) coated glass substrates, where a TiO_2 blocking layer (80 nm thick) and a TiO_2 mesoscopic layer (400 nm thick) were used, respectively. The samples were arranged on the table 1 mm below the inkjet printhead, and printed by a piezoelectric driven flatbet inkjet printer, as reported previously.[35] The printing ink consisted of MAI, PbI_2, and MACl with a molar ratio of 1-x:1:x (x=0~0.9), dissolved in γ-butyrolactone with a concentration of 35 wt%. During the printing, the samples were in situ heated on the platen at a fixed temperature in ambient conditions. After the inkjet printing, the samples were transferred into a N_2-filled glove-box for post annealing. Finally, 2,2′,7,7′-tetrakis-(N,N-di-p-methoxyphenylamine)-9,9′-spirobifluorene (spiro-OMeTAD) was deposied as a hole transport layer, followed by evaporation of a gold back electrode. Full experimental details on the device fabrication and characterization are to be found in the Supporting Information.

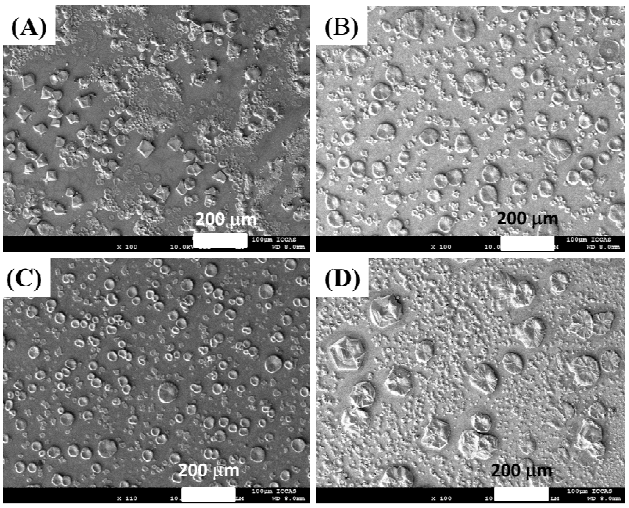

Fig.1 Top-view SEM images of inkjet printed perovskite (on mesoscopic TiO_2 films) deposited at 25 °C (a), 40 ° (b), 50 C° (c) , and 60 C° (d) .

In the printing, high boiling γ-butyrolactone (b.p.= 206 °C) was selected as solvent in the ink, on one hand, due to its high solubility for the perovskite precursor, on the other hand, preventing nozzle clogging of the printhead due to the solvent evaporation during the printing. Unlike the conventional spin coating, where most of solvent in the deposited film can be rapidly removed by centrifugal force during spin coating, the inkjet printing films, however, are usually in a fluid state, containing a large amount of solvent upon the printing. Thus, it is essential to speed up solvent evaporation from the wet film. Otherwise, the crystllization of the perovskite would be slowed down, leading to a large thickness variation of the film.[7] Thus, in situ heat treatment was applied to accelerate solvent evaporation during the printing. The table temperature was adjusted from 25 °C to 60 °C with a short duration of 2 minutes. In addition, a 400 nm thick mesoscopic TiO_2 film was used as a substrate for the perovskite printing. In this case, the printed perovskite precursor was restrained within the porous TiO_2 film after the solvent evaporation, and further converted into the crystalline perovskite with a confined nanomorphology after post-annealing.[7] It should be noted that after the printing and in situ heat treatment, the precursor on the films could not be fully converted into the crystalline perovskite. Thus, all the samples were subjected to further post-annealing for the crystallization. The process was carried out at 100 °C for 10 minutes in N_2 atmosphere after the deposition.

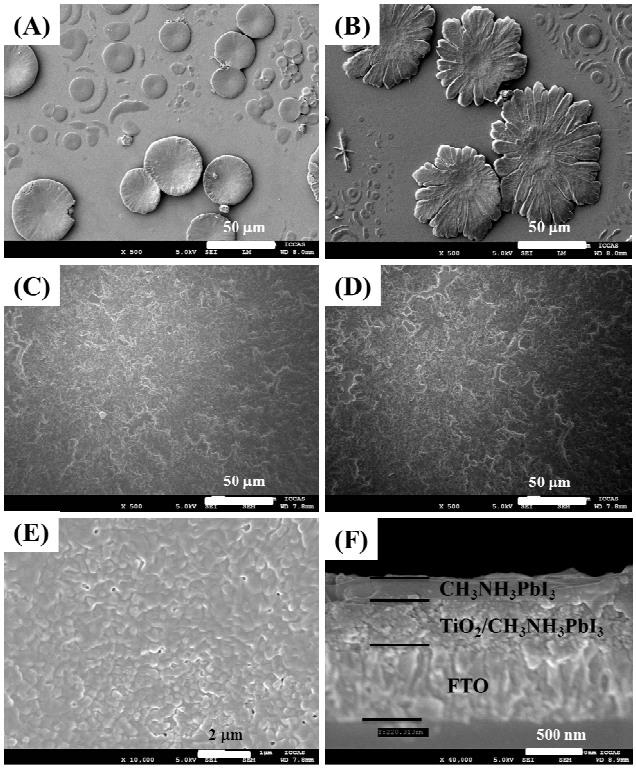

Fig.2 Top-view SEM images of mesoporous TiO_2 films coated with inkjet printing perovskite from the precursor solution with a molar ratio of 1-x:1:x for PbI_2, MAI, and MACl, respectively, at x=0 (a), x=0.3 (b), x=0.6 (c), x=0.9 (d), (e) x=0.6, the scale bar is 1 μm; and the cross-sectional SEM image at x=0.6 (f).

The influence of the table temperature on the morphology and structure of the perovskite film was examined by scanning electron microscopy (SEM). The ink used here consists of the perovskite precursor PbI_2 and MAI (molar ratio of 1:1) dissolved in γ-butyrolactone with a concentration of 35 wt%. At room temperature (25 °C), the printed film surface was intricately covered with various shapes of perovskite crystallite with distinct edges and corners, as shown in **Figure 1**. The morphology is obviously different from that of the spin coated film, where disc-like crystals were observed.[6,9] The result implies that the printed film is wet, and the precursor has more time to distribute and self-assemble at the low printing temperature, favoring the perovskite crystallization. At the temperature of 40 °C, the film morphology was changed clearly. A large amount of round and flattened crystal plates were spread uniformly on the surface, similar to that of the spin-coated film.[19] As the temperature increased to 50 °C, the crystal plates bacame larger. Meanwhile, a lot of small perovskite crystallites appeared, resulting in a relatively high substrate coverage. Further increasing the temperature to 60 °C, the plate size further increased, following with abundant pinholes

on the surface, probably due to high solvent evaporation ratio at this temperature. The pinholes can deteriorate the photovoltaic performance in the resultant devices.[19,20] The results suggested that the film morphology would strongly relate to the table temperatures, and the temperature of 50 °C would be optimal for the printing.

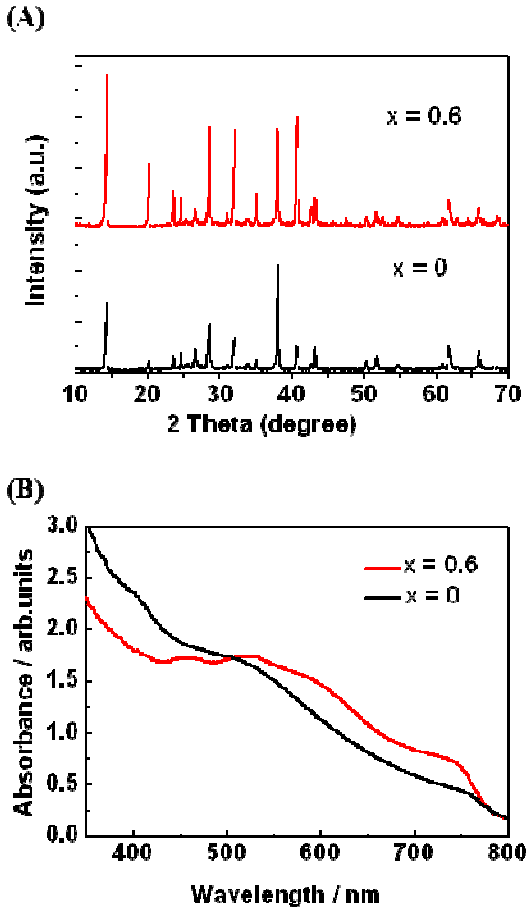

Fig.3 XRD diffraction paterns (a) and UV-vis spectra (b) of the perovskite-coated TiO_2 films prepared at x=0 and 0.6 from the precursor solution (the molar ratio of PbI_2, MAI, and MACl is 1-x:1:x)

The photovoltaic performance was measured for the devices prepared at different table temperatures. As shown in **Table 1**, **device 1** with the film deposited at room temperature (25 °C) gave a short-circuit photocurrent density (J_{sc}) of 13.21 mA cm^{-2}, an open-circuit voltage (V_{oc}) of 0.82 V, and fill factor (*FF*) of 0.61 to yield an power conversion efficiency (*PCE*) of 6.6%, which is relatively lower than those of the similar-structured devices prepared by the spin-coating method.[9] The low photovoltaic performance would come from the poor perovskite morphology with a low substrate coverage. For **device 2** with the film deposited at 40 °C, the conversion efficiency was considerably increased to 7.2%. At 50 °C deposition, **device 3** gave a *PCE* of 7.9% with a J_{sc} of 14.71 mA cm^{-2}, a V_{oc} of 826 mV and *FF* of 0.65, which is comparable to that for the device prepared by the spray-coating technique.[27] Further increasing the temperature to 60 °C for **device 4,** however, the performance slightly decreased to a *PCE* of 7.3%, probably due to the rough and pinhole-containing perovskite film leading to increased charge recombination in the device.

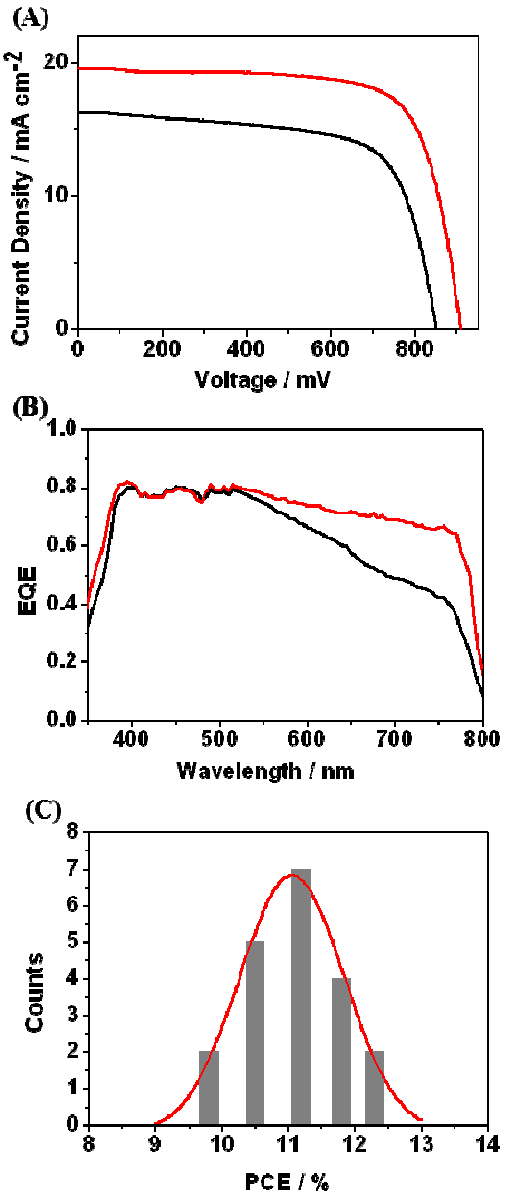

Fig.4 *I-V* curves (a) and *EQE* spectra (b) of the devices prepared the perovskite-coated TiO_2 films prepared at x=0 (black line) and 0.6 (red line), and histogram of PCEs for device 6 for 20 samples (c).

Recent reports demonstrated that the morphology of the perovskite film could be improved when halogen-containing additives were co-deposited with the perovskite presursors during the fabrication.[23-28] Here, varied amounts of the additive MACl, was added in the precursor solution for further improving the morphology of the perovskite film. In the ink, PbI_2, MAI, and MACl were mixed with a molar ratio of 1-x:1:x (x=0~0.9), and the inkjet printing was carried out at the fixed table temperature of 50 °C. We observed that the colour of the film changed from light yellow to brown during the printing, and the colour change became slow with the increase of the additive MACl in the ink.

Cite this: DOI: 10.1039/c0xx00000x

www.rsc.org/xxxxxx

ARTICLE TYPE

Table 1 Photovoltaic performance of the devices prepared at different table temperature and with various amount of CH_3NH_3Cl in the printing solution.

Device	Temperature / °C	X (CH_3NH_3Cl)	J_{sc} / mA cm^{-2}	V_{oc} / mV	FF	η / %
device 1	25	0	13.21	820	0.61	6.6
device 2	40	0	13.85	824	0.63	7.2
device 3	50	0	14.71	826	0.65	7.9
device 4	60	0	14.35	822	0.62	7.3
device 5	50	0.3	15.73	844	0.64	8.5
device 6	50	0.6	19.55	910	0.69	12.3
	50	0.6	18.91 ± 0.6	884 ± 40	0.67 ± 0.04	11.2 ± 0.7 [a)]
device 7	50	0.9	18.85	868	0.66	10.8

[a] Footnote text. The average and the standard deviation for 20 samples

previously.[24] After the printing, all the samples were post-annealed at 100 °C for 10 minutes, and the morphology was investigated by SEM. As shown in **Figure 2**, flower-like crystal plates with large size were observed upon addition of MACl at x=0.3, as compared with the disc-like crystal plates with no MACl in the ink. The flower-like crystal plates possess highly ordered internal structure, indicating a high crystallization of the perovskite when the additive was used. When x increased to 0.6, the crystals were flattened and interconnected to form a continuous uniform perovskite layer on the mesoporous TiO_2 surface with full surface coverage. The grain size in the perovskite upper layer was about 200~500 nm with the layer thickness of about 200 nm, as shown in **Figure 2f**. Further increasing x to 0.9, the perovskite film seemed to undergo partial dewetting, resulting in a relatively low surface coverage. The results indicate that the MACl additive can control the whole crystalline process and thus the morphology in the formation of the perovskite, and suitable amount of the additive is critically important for the high-quality film with good surface coverage. For further investigating the nature of the perovskite film, X-ray differaction (XRD) were conducted for the samples with the additive at x=0 and 0.6. As shown in **Figure 3**a, the XRD patterns are nearly the same for both the samples with main peaks located at 14.20, 20.08, 28.52, 31.96 and 40.66°, assigned as the (110), (112), (220), (310), and (224) planes of the tetragonal perovskite $CH_3NH_3PbI_3$ structure. indicating that the addition of the additive whould have no affection on the structure and composition of $CH_3NH_3PbI_3$. The diffraction peaks, however, became stronger in intensity upon the addition of the additive, as cmpared with those with no additive. This may be ascribed to the presence of the uniform perovskite upper layer with high crystallinity induced by the additive.[23] **Figure 3b** shows the absorption spectra of the samples at x=0 and 0.6. Clearly, the sample at x=0.6 exhibits enhanced absorbance at the long wavelength region (500-800 nm) because of the presence of the thick and high uniform upper layer as mentioned above, while the sample at x=0 shows relatively low absorbance at the region. The uniform upper layer on the mesosporous TiO_2 surface was desirable for improving the light harvesting capacity, and thus increasing device photvoltaic perfomance[6,7] In the one-step spin coating, the perovskite precursors were mainly limited in the porous TiO_2 films, and most of superfluous solution on the surface was spinned off during the deposition. Thus, it is almost impossible to controle the morphology and structure of the resultant perovskite on the porous TiO_2 film, thus exhibiting poor substrate coverage. In the inkjet printing, certain amount of the precursor solution can be well controlled as required, and completely used in the printing in principle. Thus, inkjet printing could well control the morphology and structure of the perovskite film.

To investigate the effect of the additive on the device performance, photovoltaic parameters were measured for the devices prepared with various amount of the additive MACl in the printing solution, and the results are listed in **Table 1**. As can be seen from the data, the performance of **device 5** (x =0.3) was reasonably improved with a *PCE* of 8.5% in comparison with that (7.9%) for **device 3** with no additive (x =0). At x = 0.6 for **device 6**, all the photovoltaic parameters were augmented with a J_{sc} 19.55 mA cm^{-2}, a V_{oc} of 910 mV, a *FF* of 0.69, and a *PCE* of 12.3%, which is the highest among the values for the mesoporous perovskite solar cells prepared by the standard one-step spin coating technology.[2-4] Further increasing the additives at x = 0.9 for **device 7**, however, the performance slightly decreased to 10.8%, probably due to the relatively low coverage as mentioned above. The current density-voltage (*J-V*) characteristics and the external quantum efficiency (*EQE*) spectra of **device 3** and **device 6** were shown in **Figure 4**. The difference in the efficiency mainly came from the different J_{sc}*s* in the two devices, as shown

in **Table 1** and **Figure 4a**. The external quantum efficiency (*EQE*) spectra shows that both the devices present the similar trends with the same amplitude at the short wavelength (300-500 nm), while at the long wavelength, **device 6** exhibited significantly enhanced *EQE*. The difference in the EQE spectra can be explained by the different light harvesting capacity as shown in **Figure 3b**, which is consistent with the difference in the J_{sc}s for both the devices. The results demonstrate that the uniform perovskite upper layer can effectively enhance light harvesting at long wavelength, and improve the resultant photovoltaic performance because the perovskite materials is weak absorption at long wavelength relative to the long wavelength.[6]

To check the device reproducibility, **device 6** were prepared with 20 separate samples at the same condition. As shown in **Figure 4c**, the histogram of their *PCEs* presented high reproducibility with a low relative standard variation of 6.5% and high average *PCE* of 11.2%. The high value of the average *PCE* and high reproducibility can be ascribed to the high-quality perovskite film prepared by the inkjet printing, demonstrating the great advantage of this fabrication method for the perovskite solar cells.

Conclusions

In the work reported here, inkjet printing technique was successfully used for the fabrication of flat and uniform provskite $CH_3NH_3PbI_3$ film on the mesoporous TiO_2 substrate. The role of the table temperature used in the printing was investigated, indicating that the in situ heating treatment is necessary in the printing. In addition, the CH_3NH_3Cl as an additive in the printing solution was found to have critical impact on the morphology and structure of the perovskite film formed. The film-optimized solar cell exhibited a best *PCE* of 12.3% under AM 1.5G conditions, with high reproducibility (relative standard variation of 6.5%). The current work demonstrates that the inkjet printing can be an efficient and low cost approach for large-scale production of the perovskite solar cells. Meanwhile, the inkjet printing is environmentally sound technique for the fabrication of the perovskite solar cells. Further optimization, including device configuration and printing parameters, should improve the device performance, and the researches are now under investigation.

Experimental

Synthesis of CH_3NH_3I: 10 ml of hydroiodic acid (55-58 wt %) was added dropwise to 24 ml of methylamine (33 wt%) and 100 ml ethanol under nitrogen atmosphere. A rotary evaporator was used to remove the solvent and crystallize methylammonium iodide (MAI). The precipitate was washed with diethyl ether three times. The resulting white powder was dried at 65°C in vacuum overnight.

Synthesis of CH_3NH_3Cl: 19 ml of hydrochloride acid (33 wt%) was added dropwise to 24 ml of methylamine (33 wt%) and 100 ml ethanol under nitrogen atmosphere. A rotary evaporator was used to remove the solvent and crystallize methylammonium chloride (MACl). The precipitate was washed with diethyl ether three times. The resulting white powder was dried at 65°C in vacuum overnight.

Fabrication of perovskite-based solar cells: F-doped SnO_2 (FTO) coated glass were patterned by etching with zinc powder and 2 M hydrochloric acid. The substrates were carefully cleaned in ultrasonic baths of detergents, deionized water, acetone and ethanol successively. A compact TiO_2 blocking layer was deposited onto the surface of the cleaned FTO substrate by spin-coating of titanium diisopropoxide bis(acetylacetonate) solution (0.15 M, in 1-butanol) at 4000 r.p.m. for 30 s, dried at 125 °C for 5 min, then repeated twice with 0.3 M of titanium diisopropoxide bis(acetylacetonate) solution, followed sintering on a hotplate at 500 °C for 30 min. After cooling to room temperature, the films were immersed in 0.02 M aqueous $TiCl_4$ at 70 °C for 30 min, followed by washing with ethanol and further sintering at 500 °C for 30 min. The mesoporous TiO_2 films were fabricated by spin-coating a 20 nm-sized TiO_2 dispersion solution, which was prepared by diluting a commercial paste (18NR-T, Dyesol) by ethanol at 1:3.5 by weight. A 400 nm thick layer of TiO_2 was achieved via spin coating at 3000 rpm for 30 s, followed further sintering at 500 °C for 30 min. The perovskite films were inkjet printed by the perovskite precursor solution (35 wt% in γ-butyrolactone) with a molar ratio of 1-x:1:x for PbI_2, MAI, and MACl, respectively. The inkjet printing was performed by a Dimatix Fujifilm DMP-2831 printer, including a piezoelectric-driven inkjet head with a motorized xyz stage. The printing frequency was set at 5.0 kHz and a customized waveform was used with a maximum voltage of 22 V and a pulse width of 8.5 μs. Mesoporous TiO_2 substrates were held on the platen at fixed temperatures ranging from 25 °C to 60 °C with 30–40% relative humidity (RH) in the printing chamber. After the deposition, the samples were transferred to a nitrogen-filled glovebox (<1 ppm O_2 and H_2O) for post-annealing. On the perovskite film, a layer of a hole transporting material was deposited by spin coating (4000 rpm, 30 s) a spiro-MeOTAD (2,2′,7,7′-tetrakis(*N*,*N*-di-*p*-methoxyphenylamine)-9,9-spirobifluorene) solution in a N_2-filled glovebox. The spin-coating formulation was prepared by as follows: In 1 ml chlorobenzene was added spiro-MeOTAD 75 mg, 30 μl 4-tert-butylpyridine, 20 μl of a stock solution of 500 mg ml^{-1} Li-TFSI in acetonitrile. Finally, an 80 nm thick Au was thermally evaporated as a back contact under vacuum of 3×10^{-5} Torr. The device active area was 4 mm^2, determined by the overlap of the cathode and anode.

Characterization: XRD patterns were recorded by using an X-ray diffractometer (Rigaku, D/MAX RINT-2500) with a CuKa radiation source. The surface morphology of the films as well as cross-section was analyzed by using a JEM-7500F field-emission scanning electron microscope (SEM). Absorption spectra of the film samples were recorded by using a Shimadzu Uv/Vis 1800 spectrophotometer. Current-Voltage characteristics were recorded by applying an external potential bias to the cell while recording the generated photocurrent with a Keithley model 2400 digital source meter. The light source was a 300 W collimated xenon lamp (Newport) calibrated with the light intensity to 100 $mW\cdot cm^{-2}$ at AM 1.5 G solar light condition by a certified silicon solar cell. The *J-V* curve was recorded by the reverse scans with a rate of 200 mV/s. The external quantum efficiency (EQE) for solar cells were performed using a commercial setup (PV-25 DYE, JASCO). A 300 W Xenon lamp was employed as light source for

generation of a monochromatic beam. EQE spectra were recorded using monochromatic light without white light bias. Calibrations were performed with a standard silicon photodiode. EQE is defined by EQE(λ) = $hcJ_{sc}/e\varphi\lambda$, where h is Planck's constant, c is the speed of light in a vacuum, e is the electronic charge, λ is the wavelength in meters (m), J_{sc} is the short-circuit photocurrent density (A m^{-2}), and φ is the incident radiation flux (W m^{-2}).

Notes and references

[a] *Key Laboratory of Green Printing, Institute of Chemistry, Chinese Academy of Sciences,Beijing, 100190, China*
E-mail: kjjiang@iccas.ac.cn, ylsong@iccas.ac.cn
[b] *School of Chemical Engineering and Technology, Tianjin University, Tianjin, 300072, China*
E-mail: zhouxueqin@tju.edu.cn

1 A. Kojima, K. Teshima, Y. Shirai, T. Miyasaka, *J. Am. Chem. Soc.* 2009, **131**, 6050.
2 M. M. Lee, J. Teushcer, T. Miyasaka, T. N. Murakami, H. J. Snaith, *Science* 2012, **338**, 643.
3 H. S. Kim, C. R. Lee, J. H. Im, K. B. Lee, T. Moehl, A. Marchioro, S. J. Moon, R. Humphry-Baker, J. H. Yum, J. E. Moser, M. Grätzel, N. G. Park, *Sci. Rep.* 2012, **2,** 591.
4 L. Etgar, P. Gao , Z. Xue , Q , Peng , A. K. Chandiran , B. Liu , M. K. Nazeeruddin , M. Grätzel, *J. Am. Chem. Soc.* 2012, **134**, 17396.
5 J. H. Noh, S. H. Im , J. H. Heo, T. N. Mandal, S. I. Seok, *Nano Lett.* 2013, **13**, 1764.
6 J. H. Heo , S. H. Im , J. H. Noh , T. N. Mandal, C. S. Lim , J. A. Chang ,Y. H. Lee , H. J. Kim , A. Sarkar , M. K. Nazeeruddin , M. Grätzel, S. I. Seok, *Nature Photon.* 2013, **7**, 486.
7 J. Burschka, N. Pellet, S. J. Moon, R. Humphry-Baker, P. Gao , M. K. Nazeeruddin, M. Grätzel, *Nature* 2013, **499**, 316.
8 M. Liu, M. B. Johnston, H. J. Snaith, *Nature* 2013, **501**, 395.
9 J. H. Noh, S. H. Im, J. H. Heo, T. N. Mandal, S. I. Seok, *Nano Lett.* 2013, **13**, 1764.
10 J. M. Ball, M. M. Lee, A. Hey, H. Snaith, *Energy Environ. Sci.* 2013, **6**, 1739.
11 D. Liu, T. L. Kelly, *Nature Photon.* 2014*,* **8***, 133.*
12 Q. Chen, H. Zhou, Z. Hong, S. Luo, H. S. Duan, H. H. Wang, Y. Liu, G. Li, Y. Yang, *J. Am. Chem. Soc.* 2014, **136**, 622.
13 Z. Xiao, C. Bi, Y. Shao, Q. Dong, Q. Wang, Y. Yuan, C. Wang, Y. Gao, J. Huang, *Energy Environ. Sci.* 2014, **7**, 2619.
14. NREL (http://www.nrel.gov/ncpv/images/efficiency_chart.jpg), accessed on Oct. 15, 2014.
15. H. Zhou, Q. Chen, G. Li, S. Luo, T. Song, B. H. S. Duan, Z. Hong, J. You, Y. Liu, Y. Yang, *Science* 2014, **345**, 542.
16 S. D. Stranks, G. E. Eperon, G. Grancini, C. Menelaou, M. J. P. Alcocer, T. Leijtens, L. M. Herz, A. Petrozza, H. J. Snaith, *Science* 2013, **342**, 341.
17 G. Xing, N. Mathews, S. Sun, S. S. Lim, Y. M. Lam, M. Grätzel, S. Mhaisalkar, T. C. Sum, *Science* 2013, **342**, 344.
18 C-W. Chen, H-W. Kang, S-Y. Hsiao, P-F. Yang, K-M. Chiang, H-W. Lin, *Adv. Mater.* DOI:10.1002/adma.201402467.
19 B. Conings, L. Baeten, C. D. Dobbelaere, J. Dhaen, J. Manca, H-G. Boyen, *Adv. Mater.* 2014, **26**, 2041.
20 A. Dualeh, N. Tétreault, T. Moehl, P. Gao, M. K. Nazeeruddin, M. Grätzel, *Adv. Func. Mater.* 2014, **24**, 3250.
21 P. Liang, C-Y. Liao, C-C. Chueh, F. Zuo, S. T. Williams, X-K. Xin , J. Lin , A. K.-Y. Jen, *Adv. Mater.* 2014, **26**, 3748.
22 N. J. Jeon, J. H. Noh, Y. C. Kim, W. S. Yang, S. Ryu, S. I. Seok, *Nature Mater* 2014, **13**, 897.
23 Y. Zhao, K. Zhu, *J. Phys. Chem. C*, 2014, **118**, 9412.
24 P-W. Liang, C-Y. Liao, C-C. Chueh, F. Zuo, S.r T. Williams, X-K. Xin, J. Lin, A.K.-Y. Jen, *Adv. Mater.* 2014, **26**, 3748.
25 C. Zuo, L. Ding, *Nanoscale*, 2014, **6**, 9935.
26 H. Yu, F. Wang , F. Xie, We. Li , J. Chen, N. Zhao, *Adv. Funct. Mater.* DOI: 10.1002/adfm.201401872.
27 H. Zhou, Q. Chen, G. Li, S. Luo, T-B. Song, H-S. Duan, Z. Hong, J. You, Y. Liu, Y. Yang, *Science* 2014, **345**, 542.
28 P. Docampo, F. Hanusch, S. D. Stanks, M. Döblinger, J. M. Feckl, M. Ehrensperger, N. K. Minar, M. B. Johnston, H. J. Snaith, T. Bein, *Adv. Energy. Mater.* DOI:10.1002/aenm.201400355.
29 A. T. Barrows, A. J. Pearson, C. K. Kwak, A. D. F. Dunbar, A. R. Buckley, D. G. Lidzey, *Energy Environ. Sci.*, 2014, **7**, 2944.
30 Z. Wei, H. Chen, K. Yan, S. Yang, *Angew. Chem.* DOI: 10.1002/ange.201408638.
31 M. Singh, H. M. Haverinen, P. Dhagat, G. E. Jabbour, *Adv. Mater.* 2010, **22**, 673.
32 E. Tekin, H. Wijlaars, E. Holder, D. A. M. Egbe, U. S. Schubert, *J. Mater. Chem.* 2006, **16**, 4294.
33 C. N. Hoth, S. A. Choulis, P. Schilinsky, C. J. Brabec, *Adv. Mater.* 2007, **19**, 3937.
34 Y.-Y. Noh, N. Zhao, M. Caironi, H. Sirringhaus, *Nat. Nanotechnol.* 2007, **2**, 784.
35 Z. Zhang, X. Zhang, Z. Xin, M. Deng , Y. Wen, Y. Song*, Adv. Mater.* 2013*,* **25**, 6714.

Shao-Gang Li,Ke-Jian Jiang,* Mei-Jue Su, Xue-Ping Cui, Jin-Hua Huang, Qian-Qian Zhang, Xue-Qin Zhou,* Lian-Min Yang, Yan-Lin Song*

Inkjet Printing $CH_3NH_3PbI_3$ on Mesoscopic TiO_2 Film for Highly Efficient Perovskite Solar Cells

Perovskite $CH_3NH_3PbI_3$ is deposited as a light absorber on a mesoporous TiO_2 film by inkjet printing technology, and the structure and morphology are investigated with different table temperatures and with various amounts of CH_3NH_3Cl additive in the printing. The optimized device exhibits a highest power conversion efficiency of 12.3% with an average value of 11.2% under AM 1.5G conditions.